

Clay Information Extraction based on SAM of ASTER SWIR Image

Cheng bo

Associate Professor, Ph. D , China Remote Sensing
Satellite Ground Station, Chinese Academy of Sciences
#45, Bei san huan xi Road, Beijing, 100086
Tel:(86)-10-62552480 Fax:(86)-10-62561215
E-mail: bocheng@ne.rsgs.ac.cn

KEY WORDS: Clay, SAM, ASTER, Dexing

ABSTRACT: The extensive clayization of Dexing copper mine is responsible for water and soil pollutions because of the oxidation of sulfide minerals. During the clayization, harmful elements such as As, S, Sb and Pb could be effectively released into the clay and water. Using the abundant spectral information of short wave infrared (SWIR), combining with the spectral absorbed index, SAM (Spectrum Angle Mapper) which based on spectral matching, subtly compartmentalizes the degree of clay and distribution in copper mine.

1. Introduction

Adverse impacts of heavy metal pollution, originating from mining, smelting and manning activities, on the aquatic ecosystem of Dexing Copper Mine in south China, is evaluated by integrating the chemical, toxicological and ecological responses of single and multiple metals in overlying water, surface sediment and floodplain topsoil. The assessment results indicated that a highly localized distribution pattern was closely associated with the pollution sources around the mine. The extensive clayization of Dexing copper mine is responsible for water and soil pollutions because of the oxidation of sulfide minerals. During the clayization, harmful elements such as As, S, Sb and Pb could be effectively released into the clay and water to result in water and soil pollutions because of the oxidation of sulfide minerals such as pyrite, arsenopyrite, stibnite, galena, and sphalerite. Clayization is a major environmental factor in many mines.

While not a typical hyperspectral sensor system, ASTER does provide substantial improvements over the traditional multispectral sensor, such as Landsat thematic mapper (TM), in spatial, spectral and radiometric resolutions. To many researchers, ASTER has become a vital data source for geological mapping because of resolution improvements and the free-of-cost data availability. This is especially true given the possible interrupted availability of Landsat TM/ETM+ sensor data in 2004. Because of their broad spectral band passes, Landsat TM images cannot identify specific alteration minerals, such as jarosite, alunite and individual clay minerals. Techniques for the digital enhancement of Landsat TM data for mapping hydrothermally altered zones aim at the identification of clay (Crosta and Rabelo, 1993). Carranza and Hale (2002) suggested that, Landsat TM bands 5 and 7 are potentially useful in detecting clay zones in arid area. Similarities in shape and

relative intensities of the reflectance curves of vegetation and clay minerals in the spectral regions covered by Landsat TM bands 5 and 7 make their discrimination difficult.

The objective of this paper is to employ spectral image processing techniques that have been used often to process hyperspectral data to analyze ASTER data for the purpose of mapping clay units in Dexing copper mine, with the hope that these techniques will make effective use of the richer information content furnished by ASTER's relatively high spectral resolution. The following section is devoted to introducing the geology of the study area (Dexing copper mine), followed by a description of the ASTER sensor system and the remote sensing dataset used in this research. The spectral image analysis techniques applied to the ASTER dataset are then explained and the results are described. Finally, these results are discussed in terms of their geological implications.

2. Study area and data acquisition

2.1 Study area

The Dexing district in Jiangxi Province is the largest porphyry copper orefield in China and contains 1500 Mt ore at 0.43% Cu, 0.02% Mo, 0.16 g/t Au and 1.9 g/t Ag, approximately equivalent to 6.45 Mt Cu, 0.25 Mt Mo, 24 t Au and 285 t Ag (Yan and Hu, 1980; 1999; He et al., 1999). The Dexing deposits are associated with granodiorite porphyries of Yanshanian age (148–170 Ma) that intruded slate and phyllite of the Mesoproterozoic Shuanqiaoshan Group. The granodiorite porphyries lie along the intersection of a NW trending fault and NE trending anticlinal axis. The three orebodies, Tongchang, Fujiawu and Zhushahong are pipe-like in profile and circular in plan, with the largest, Tongchang, being 0.7 km in diameter. The contact zone between the porphyry and the host rocks is metamorphosed to hornfels. Two thirds of the copper reserves in the Tongchang deposit are in the country rock and the contact zone. The ore minerals are pyrite, chalcopyrite, molybdenite, tennantite, bornite, and electrum.

The Le'an River is located at north of Dexing copper mine. It receives a large amount of acidic mine drainage (pH 2–3) and waste effluents containing Cu, Pb and Zn discharged from the neighboring Dexing Cu Mine (ore production of 105 tons per day) and from many smelters and mining/panning activities along the banks of mainstream and tributaries. Great input of clay and distribution in different bound phases has led to a severe deterioration in the surrounding environments. The main objective of this study is to delineate the distribution and extent of clay pollution.

2.2 Field spectroradiometric data

The spectroradiometer used on the ground is a high spectral resolution analytical spectral device (ASD). It operates in the visible, the near infrared and the shortwave infrared (350–2500 nm). The radiometric measurements were carried out with resolution intervals of 10 nm between 350 and 1000 nm and 20 nm between 1000 and 2500 nm. This position permits the vertical viewing of a circular surface with a radius

of approximately 25 cm. A spectral onboard served as reference before and after each measurement. The objective of this procedure is to minimize errors due to variations in atmospheric conditions and sun inclination. The bidirectional effects of the target reflectance were accounted for by carrying out measurements over very short and close time intervals and by keeping the viewing angle constant and in a vertical position (Mohamed et al. 2005) .

The measurement campaign was conducted between 18 and 24 November 2000. The choice of the measurement sites is based on the soil, geological and topographic maps and our knowledge of the study area so as include most of the surface conditions or the different levels of clayization. Reflectance curves give useful diagnostic information on their elemental and mineralogical composition. This is because the various alteration minerals have distinctive absorption and radiance features caused by the presence of OH, Si-O and other hydroxyl bonds Mg-OH, Al-OH, particularly in the SWIR. According to Ferrier et al. (2002), clayization usually appears at deeper absorption in 2200nm. It is a clay-rich type of alteration in field(Fig 1).

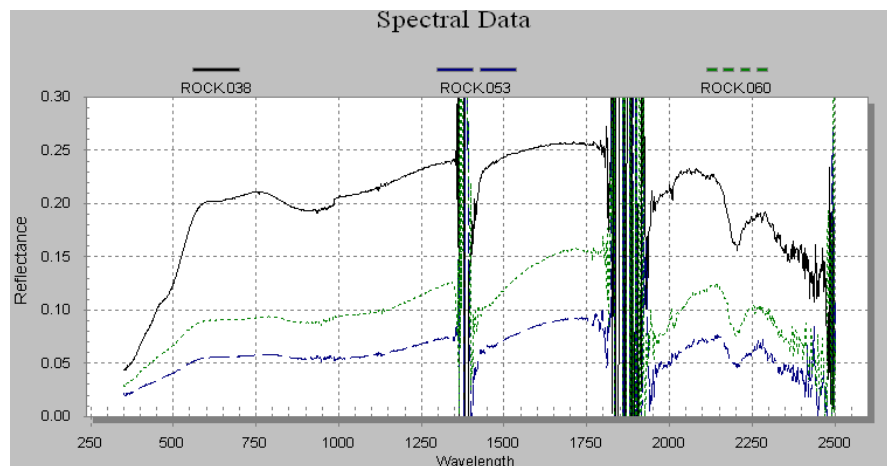


Fig.1 Spectral curves of the clay-rich point in Dexing copper mine

2.3 ASTER data and preprocessing

ASTER is a multi-spectral imaging radiometer installed on the Terra platform in 1999. It is the result of a collaborative effort between NASA and the Japanese Ministry of Economy Trading and Industry (METI), formerly known as the Ministry of International Trade and Industry (MITI). The ASTER sensor is equipped with a stereoscopic acquisition mode permitting the extraction of digital terrain models. It has 14 bands with a spectral resolution varying from 0.52 to 11.65 nm. The sensor itself is equipped with three separate radiometers (Abrams, 1997). They cover respectively the three following portions of the spectral domain: the visible and the near infrared (NIR), the shortwave infrared (SWIR) and the thermal (Table 1). This study covers only VNIR and SWIR spectral bands, and the TIR spectral bands of ASTER were not used.

Table 1
ASTER sensor characteristics

VNIR (μm)	SWIR (μm)	TIR (μm)
Bands		
B1: 0.520–0.600 (Nadir)	B4: 1.600–1.700	B10: 8.125–8.475
B2: 0.630–0.690 (Nadir)	B5: 2.145–2.185	B11: 8.475–8.825
B3N: 0.760–0.860 (Nadir)	B6: 2.185–2.225	B12: 8.925–9.275
B3B: 0.760–0.860 (\pm inclined by 24°)	B7: 2.235–2.285	B13: 10.250–10.950
	B8: 2.295–2.365	B14: 10.950–11.650
	B9: 2.360–2.430	
Spatial resolution (m)		
15	30	90

The ASTER sensor is characterized by a repeat cycle of 16 days and provides a scene of the order of 60 kmX60 km. It follows the same orbit as Landsat 7 but 30 min later. The ASTER scene used for the study was acquired during the month of June 2002. It corresponds to level AST_2B05, which contains the surface reflectance. The image was corrected atmospherically and radiometrically by the image provider. The geometric correction was carried out using a polynomial approach. We applied a correction to the image in relation to the 1:50,000 topographic map covering the study area. The transfer equation is a first degree polynomial function calculated from the control points. Resampling was carried out using the nearest neighbor method so as not to severely alter the pixel values. Using the least squares method, the correction accuracy was determined by calculating the residual errors between the value obtained by the application of the function and the true value.

Diagnostic spectral features for clay minerals are found in the six SWIR bands, which therefore have the potential to map important alteration minerals.

3. Methods

As is showed by Fig.2, any spectral reflectance characteristics can be composed of spectral absorption valley and two shoulders of spectral absorption S_1 , S_2 . According to remote sensing image's spectral resolution and central wavelength position, S_1 , S_2 , M can respectively be image of one band and can also be linear combination of several bands. The distance of "non-absorption baseline" (dashed line in image) composed of absorption valley point M and the two shoulders can be characterized as spectral absorption depth (H).

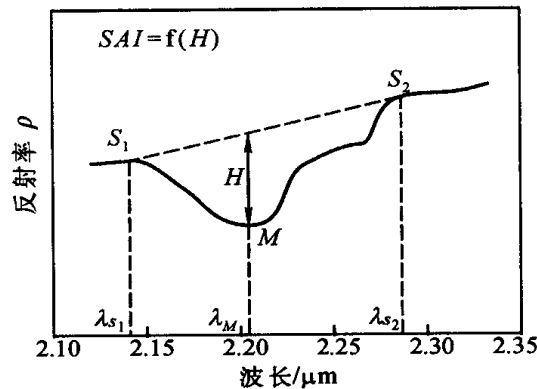


Fig.2 The concept plan of spectral absorption index (Wang jinnian, etc, 1996)

Spectral Angle Mapping (SAM) is a measurement of material spectral waveform comparability degree (Kruse et al., 1993). It is a self-based spectral classification, consider every stripe of spectrum as a vector in Spectrum Space, by calculating the vector angle of measurement spectra and reference spectrum to determinate the similarity strength of the two spectrums. The smaller the vector angle, the greater the similarity degree of measurement spectrum and reference spectrum, the material represented by measurement spectrum is the same or similar degree with reference spectrum material (Fig. 3). Spectral angle has better noise immunity to multiplier interference, is not affected by the changes of illumination, etc. It uses all the scene bands. The method determines the similarity between the reference spectrum and the image spectrum by the calculation of the angle.

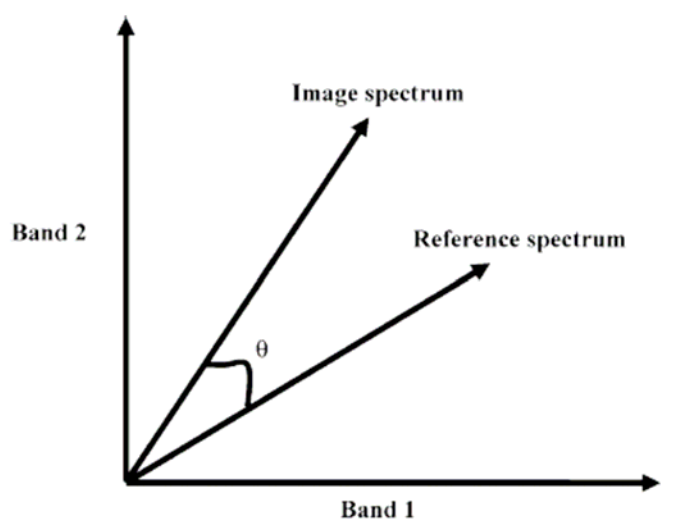


Fig.3. Spectral angle between the reference spectrum and the image spectrum in a bidimensional space (Kruse et al., 1993).

In the abnormal extraction of spectral angle of multi-spectra remote sensing, the reference spectrum may select the typical spectrum, the ground-survey spectrum or the pixel spectrum. Pixel spectral curve refers the broken line composed of pixel values of each band. The spectral analysis according to pixels' spectrum are used to calculate the included angle between every pixel spectrum in image and that of abnormal areas (known polluted areas) and to measure the degree of similarity between them. So in essence the method is one of supervised classification methods. It only considers the degree of similarity of the pixel spectral curve's shape, while basically not consider its absolute value. Moreover it only considers the similar degree with the known pixel, without considering whether the pixel is similar to others.

The approach considers the pixel values as a vector in a space with a size equal to the number of bands. The attribution of each scene pixel to a given class by the SAM approach is based on the measurement of the angle between the reference spectrum vector and each image vector. The implementation of the SAM approach gives an image with an angle for each reference spectrum. Using the angle images, we

carried out a thresholding to attribute the theme that has the lowest α value to each pixel; the smaller the angular difference, the higher is the similarity.

SAM is a method designed for a spectral space of n-dimensions and available in the ENVI image analysis software. In fact, ASTER data are used for the first time with this method for mapping clayization.

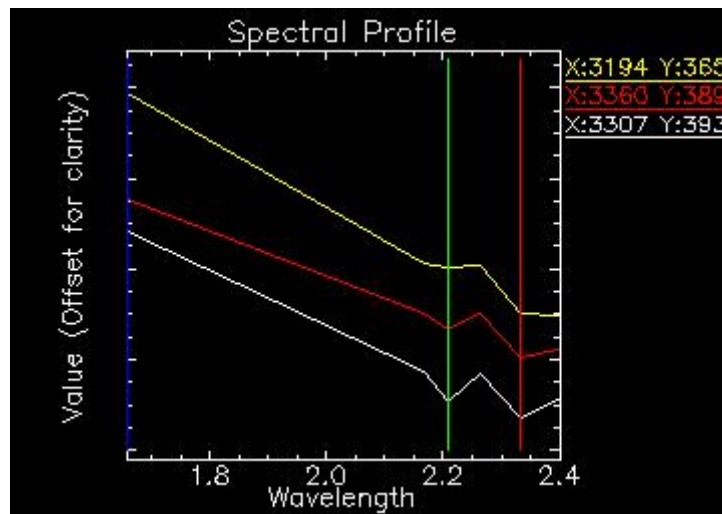


Fig. 4 Sampling point of clayization at ASTER-SWIR band

4. Results

The survey in the wild found that the pollution of mine exposed area includes the abnormal degree of clayization. The long-term weathering or heap leaching function to the copper mining rock and abandoned rock field in the open air may cause clayization. Bands of ASTER image which is close to clayization are short-wave infrared bands-5, 6, 7. The band 6 (2209nm) is the absorption valley, while band 5 (2169nm) and band 7 (2263nm) are reflex shoulder, similar to the sketch of spectral absorption index (fig.2). In practical application, collect terminal pixel in SWIR as the known regional abnormally according to the corresponding point measured from the field(fig.4). The absorption characteristic of clay can be seen obviously through the spectrum curve of white pixel. The depth of absorption is big in 2200nm, followed by the red line, yellow line basically has no absorption characteristics. The degree of similarity between every pixel in image and the known curve can be calculated according to the spectral absorption principle with SAM classification, that can be effectively in detection of polluted area caused by clayization. We have carried on the correlation match to the serious pollution area, the medium pollution area and the non-pollution area. As a result we get a SAM classification image (Fig.5) and the largest fitting angle is 0.05. The white represents the serious clay-polluted area, mainly concentrates in the Zhujia, Xiyuan abandoned rock field and Fujiawu mud-rock flow basin. The red represents the weak polluted area, displays in the open cut mining area, Fujiawu abandoned mine and NO.4 tailings. The yellow represents the non-polluted area, mainly distributes in Dawu river's coast, and tailings such as NO.1,

NO2. But these areas have a certain concentration of iron oxide. The rest areas' mask are black.

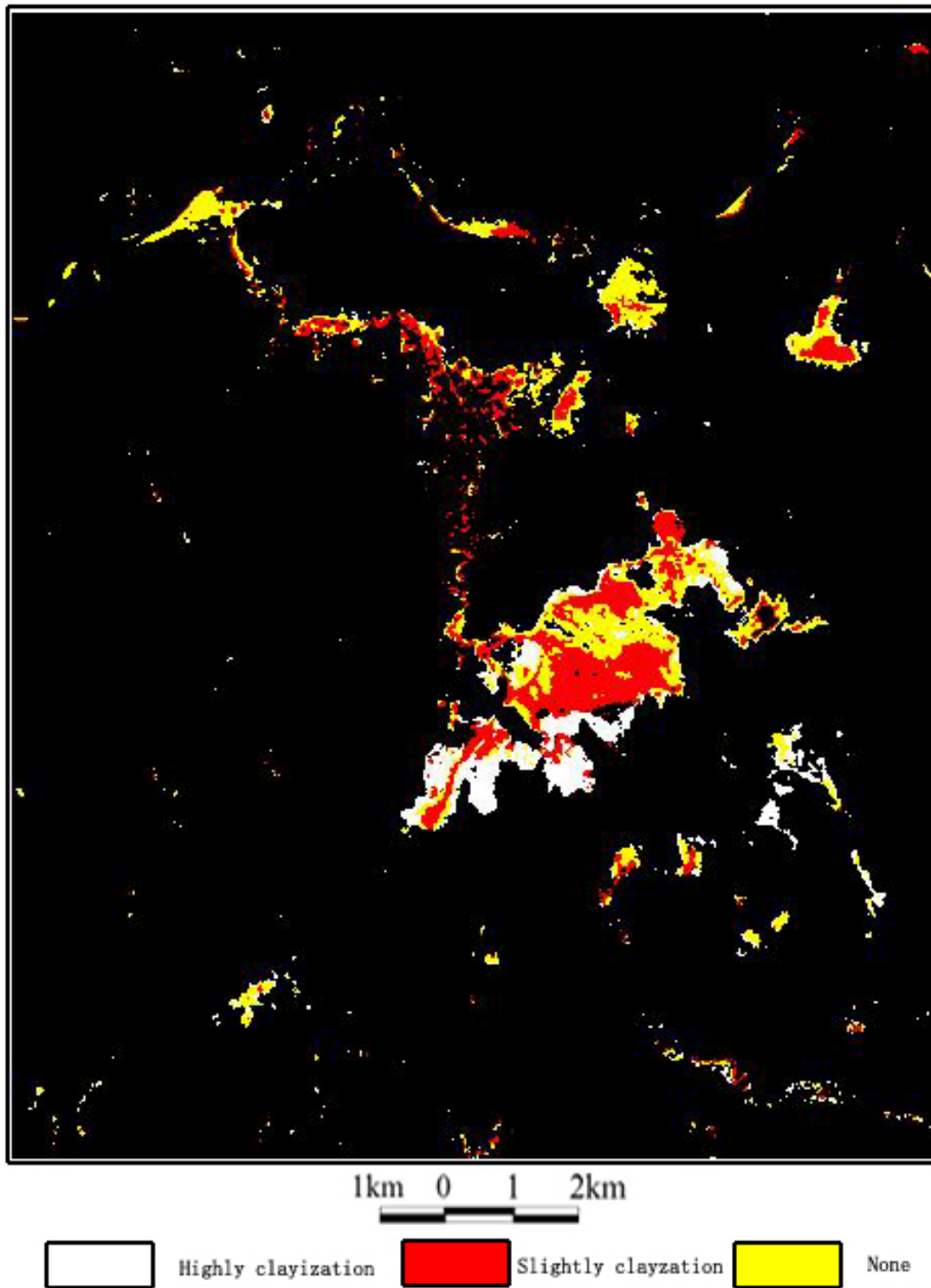


Fig5 SAM classification image for clayization

As the former, the same polluted state can be found from the color image synthesized by three bands(band7, band6 and band5) of SWIR. The accuracy of supervised was proved. In the image, the clayization levels of Zhujia, Xiyuan deserted stone mill and Fujiawu mud-rock flowing areas which are in fresh pink were high,

while the clayization levels of coarse mining sand in main open pit quarry, Fujiawu deserted mining area and the outside of the 4th cave which are in light pink were low. Additionally, there didn't exist clayization in Dawu riverside and estuary, the 1st and the 2nd cave practically, and the main pollution materials were iron oxides. This was consistent with the result of actual measuring spectrum curves (Fig.1).

5. Conclusions

The extensive clayization of Dexing copper mine is responsible for water and soil pollutions because of the oxidation of sulfide minerals. Reflectance curves by field spectroradiometric data give useful diagnostic information on clayization. Using the abundant spectral information of ASTER SWIR, combining with the spectral absorbed index, SAM which based on spectral matching, subtly compartmentalizes the degree of clay and distribution in copper mine.

As one of the recent developments in remote sensing technology, ASTER data provide not only improved spatial and radiometric resolutions, but also much richer spectral information content when compared with traditional multiple spectral remote sensing data such as Landsat TM/ETM+. The open availability of ASTER data with an associated minimal cost makes it a very attractive choice for many earth science researchers.

References

- Abrams, M., 1997. The advanced spaceborne thermal emission and reflection radiometer ASTER: data products for the high spatial resolution imager on NASA's Terra platform. *Int. J. Rem. Sens.* 21, 847–859.
- Carranza, E.J.M., Hale, M., 2002. Mineral imaging with Landsat Thematic Mapper data for hydrothermal alteration mapping in heavily vegetated terrane. *International Journal of Remote Sensing* 23, 4827 - 4852.
- Crosta, A.P., Rabelo, A., 1993. Assessing Landsat TM for hydrothermal alteration mapping in central-western Brazil. In: Boardman, J.W. (Ed.), *Proceedings of the Ninth Thematic Conference on Geologic Remote Sensing*, vol. II. Pasadena, California, USA, pp. 1053 - 1061.
- Ferrier, G., White, K., Friffiths, G., Bryant, R., Stefouli, M., 2002. The mapping of hydrothermal alteration zones on the island of Lesbos, Greece using an integrated remote sensing dataset. *Int. J. Remote Sens.* 23, 341–356.
- Gillespie, A.R., Matsunaga, T., Rokugawa, S., Hook, S.J., 1998. Temperature and emissivity from advanced space-borne Thermal Emission and Reflection Radiometer (ASTER) images. *IEEE Transactions on Geoscience and Remote Sensing* 36, 113 - 1126.
- He, W., Zhengyu, B., Tieping, L., 1999. One-dimensional reactive transport models of alteration in the Tongchang porphyry copper deposit, Dexing district, Jiangxi Province, China. *Economic Geology* 94, 307 - 323.

Kruse, F.A., Lefkoff, A.B., Boardman, J.W., Heidebrecht, K.B., Shapiro, P.J., Goetz, A.F.H., 1993. The spectral image processing system (SIPS)-interactive visualisation and analysis of imaging spectrometer data. *Rem. Sens. Environ.* 44, 145–163.

Mohamed Chikhaoui, Ferdinand Bonn, Amadou Idrissa Bokoye, Abdelaziz Merzouk. 2005. A spectral index for land degradation mapping using ASTER data: Application to a semi-arid Mediterranean catchment. *International Journal of Applied Earth Observation and Geoinformation* 7:140–153.

Wang Jinnian, Zheng Lanfen, Tong Qingxi. Spectral absorption identification model and mapping mineral mapping by airborne high spectral resolution remote sensing data. In *Proceedings of Eleventh Thematic Conference and Workshop on Applied Geologic Remote Sensing Las Vegas, Nevada r February 1996*: 27~ 29.

Yan, M.Z., Hu, K., 1980. Geological characteristics of the Dexing porphyry copper deposits, Jiangxi, China. *Mining Geology Special Issue* 8, 197 - 203.